Results in Physics 28 (2021) 104598

Contents lists available at ScienceDirect

Results in Physics

journal homepage: www.elsevier.com/locate/rinp

Mathematical model of COVID-19 in Nigeria with optimal control

Adesoye Idowu Abioye [a], Olumuyiwa James Peter [a], Hammed Abiodun Ogunseye [b], Festus Abiodun Oguntolu [c], Kayode Oshinubi [d], Abdullahi Adinoyi Ibrahim [e], Ilyas Khan [f,*]

[a] Department of Mathematics, University of Ilorin, Ilorin, Nigeria
[b] Department of Mathematics, University of Lagos, Nigeria
[c] Federal University of Technology Minna, Niger State, Nigeria
[d] AGIES Research Unit, Université Grenoble Alpes, France
[e] Department of Mathematical Sciences, Baze University Abuja, Nigeria
[f] Department of Mathematics, College of Science Al-Zulfi, Majmaah University, Al-Majmaah 11952, Saudi Arabia

ARTICLE INFO

Keyword:
COVID-19
Model-fitting
Basic reproduction number
Global stability
Optimal control

ABSTRACT

The novel Coronavirus Disease 2019 (COVID-19) is a highly infectious disease caused by a new strain of severe acute respiratory syndrome of coronavirus 2 (SARS-CoV-2). In this work, we proposed a mathematical model of COVID-19. We carried out the qualitative analysis along with an epidemic indicator which is the basic reproduction number ($\mathscr{R}_0$) of this model, stability analysis of COVID-19 free equilibrium (CFE) and Endemic equilibrium (EE) using Lyaponuv function are considered. We extended the basic model into optimal control system by incorporating three control strategies. These are; use of face-mask and hand sanitizer along with social distancing; treatment of COVID-19 patients and active screening with testing and the third control is prevention against recurrence and reinfection of humans who have recovered from COVID-19. Daily data given by Nigeria Center for Disease Control (NCDC) in Nigeria is used for simulation of the proposed COVID-19 model to see the effects of the control measures. The biological interpretation of this findings is that, COVID-19 can be effectively managed or eliminated in Nigeria if the control measures implemented are capable of taking or sustaining the basic reproductive number R_0 to a value below unity. If the three control strategies are well managed by the government namely; NCDC, Presidential Task Force (PTF) and Federal Ministry of Health (FMOH) or policy-makers, then COVID-19 in Nigeria will be eradicated.

1. Introduction

A novel coronavirus disease (2019-nCoV) outbreak in Wuhan City, Hubei, China was announced on December 31, 2019 by World Health Organization (WHO) [1]. On February 11, 2020, an International Committee on Taxonomy of Viruses gave the disease a name called Severe Acute Respiratory Syndrome Coronavirus 2 (SARS-CoV-2) [2]. Due to the high rate of global spread of this virus, World Health Organization declared it to be a global pandemic on March 11, 2020 [3]. As at September 7, 2020, by 10:26 h, the global confirmed cases of COVID-19 stood at 27,300, 888 (+25,452) with 893,130 (+455) that is, 3.27% deaths. United states of America (USA) had the highest number of confirmed cases of 6,460,421 (+171) with 193,253 (+3) deaths. This was followed by India which had the number of confirmed cases of 4,208,645 (+6,083) with 71,711 (+24) deaths. Brazil was the third country with the highest number of confirmed cases of COVID-19 with 4,137,606 confirmed cases and 126, 686 deaths [4]. Nigeria, Africa's most populous country with an estimated 200 million population [5], is one of the COVID-19 epicenters in Africa. On 27th February 2020, Nigeria recorded its first COVID-19 case when an Italian citizen employed in Nigeria was diagnosed with the disease when he had returned to Nigeria during his visit to Milan, Italy [6]. As of September 7, 2020, Nigeria was ranked 52nd with the highest number of confirmed cases of 55, 005 with 1,057 deaths [6]. Among other symptoms of COVID-19 are; sore throat, dry cough, fever, loss of taste, muscle pain, fatigue and cold [6]. On 24th January 2021, there was a rise in the number of confirmed case for coronavirus (COVID-19) in Nigeria, reaching a total of 142,579 confirmed cases. A total of 1,702 casualties and 118 thousand recoveries were recorded in the country as of the same date. As regards reported cases, Nigeria is the sixth top-ranked African country. The highest daily increase in cases in Nigeria since the beginning of the pandemic was reported on January 23. The Cumulative

* Corresponding author.
E-mail address: i.said@mu.edu.sa (I. Khan).

https://doi.org/10.1016/j.rinp.2021.104598
Received 9 March 2021; Received in revised form 20 July 2021; Accepted 22 July 2021
Available online 30 July 2021

number of confirmed cases of COVID-19 in Nigeria was recorded from February 28, 2020 to February 10, 2021 [7]. Over the years, mathematical models have proved to be reliable and powerful tools used to implement control measures to prevent and minimize the impact of infectious diseases [8,9].

For time series data on reported cases of COVID-19 in Nigeria, see Fig. 1. Several deterministic mathematical models have been developed to analyze the spread of COVID-19 pandemic and to improve our understanding on the transmission dynamics of the disease [10–28]. Some researchers have used Nigeria as a case study [29–31], but none has considered the combination of three control strategies.

The need to develop a mathematical model to study the dynamics of the transmission and spread of diseases with control measures is important because of the rapid spread of COVID-19 in Nigeria. This study is motivated by the "on-going" community spread of the novel disease of COVID-19 in Nigeria with a view to flattening the infection curve. In order to achieve this goal, we develop a new deterministic mathematical model with five-compartments based on the epidemiological status of individuals. In order to determine the optimal level of time-dependent prevention and management steps that will substantially reduce the number of infectious humans in the population, the optimal control strategy is used in the proposed COVID-19 model.

2. COVID-19 model formulation

In this section, we use mathematical model to illustrate the total population of humans at time t denoted by $N(t)$. The total population is subdivided into five compartments. That is, susceptible humans ($S(t)$), exposed humans ($E(t)$), humans infected with COVID-19 disease ($I(t)$), quarantine ($Q(t)$) and recovered humans from COVID-19 ($R(t)$). Therefore

$$N(t) = S(t) + E(t) + I(t) + Q(t) + R(t).$$

Λ is the recruitment rate of humans, ϕ_c is the contact rate of COVID-19 transmission. Also, υ_1 and θ are the recovery rates of COVID-19 from $I(t)$ and $Q(t)$ respectively. μ is the natural death rate, δ is the COVID-19-induced death rate. α is the detection rate from $I(t)$ and υ_2 is the relapse rate of COVID-19. Therefore, susceptible humans develop COVID-19 infection at the rate $\beta_c = \frac{\phi_c I}{N}$. The formulation above with the assumptions and the movement of human from one stage to another at different rates can be shown in the COVID-19 flow chart model in Fig. 2.The flow chart of the COVID-19 model is represented by the following differential equations written below

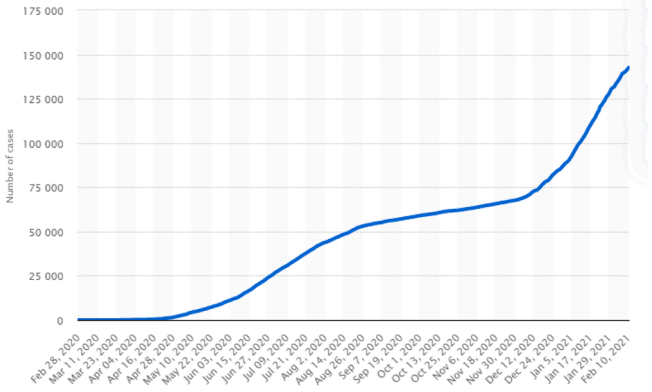

Fig. 1. Time series data on reported cases of COVID-19 in Nigeria. Source: Nigeria Center for Disease Control [7].

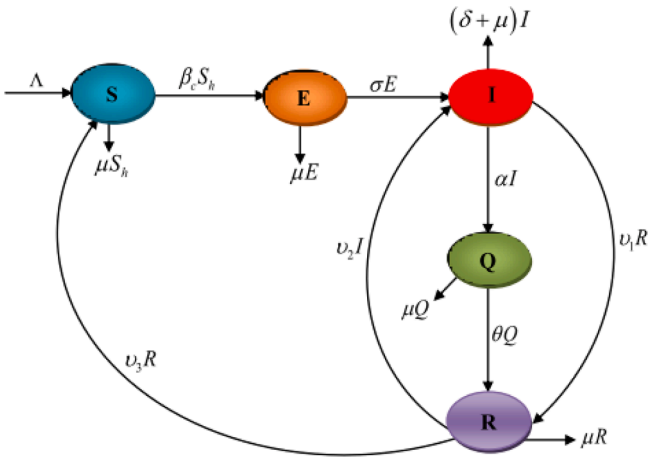

Fig. 2. Flow chart of the model.

$$\begin{aligned}
\frac{dS}{dt} &= \Lambda - \frac{\phi_c IS}{N} - \mu S + \upsilon_3 R,\\
\frac{dE}{dt} &= \frac{\phi_c IS}{N} - (\sigma+\mu)E,\\
\frac{dI}{dt} &= \sigma E - (\alpha+\upsilon_2+\delta+\mu)I + \upsilon_1 R,\\
\frac{dQ}{dt} &= \alpha I - (\theta+\mu)Q,\\
\frac{dR}{dt} &= \theta Q - (\upsilon_1+\upsilon_3+\mu)R + \upsilon_2 I.
\end{aligned} \tag{1}$$

Using $S = \frac{S}{N}, E = \frac{E}{N}, I = \frac{I}{N}, Q = \frac{Q}{N}$ and $R = \frac{R}{N}$ to normalize the eq.(1), we obtain

$$\begin{aligned}
\frac{dS}{dt} &= \Lambda - \phi_c IS - \mu S + \upsilon_3 R,\\
\frac{dE}{dt} &= \phi_c IS - (\sigma+\mu)E,\\
\frac{dI}{dt} &= \sigma E - (\alpha+\upsilon_2+\delta+\mu)I + \upsilon_1 R,\\
\frac{dQ}{dt} &= \alpha I - (\theta+\mu)Q,\\
\frac{dR}{dt} &= \theta Q - (\upsilon_1+\upsilon_3+\mu)R + \upsilon_2 I.
\end{aligned} \tag{2}$$

3. Analysis of COVID-19 model

In this section, we will carry out the quantitative study of COVID-19 which comprises the positivity and boundedness of the solutions, invariant region of the COVID-19 model and existence of equilibrium points for COVID-19 model. Others include, the basic reproduction number ($\mathscr{R}_0$) of COVID-19 model, global stability of COVID-19 free and endemic equilibria.

3.1. Positivity of the Solution

Theorem 1. *Let $S(0), E(0), I(0), Q(0), R(0)$ be non-negative initial conditions, then the solutions $(S(t), E(t), I(t), Q(t), R(t))$ of the proposed model in (2) are positive for all $t > 0$.*

Proof. Let $t^* = sup\{t > 0 : S(t), E(t), I(t), Q(t) and R(t) > 0\}$, then $t^* > 0$. From the first equation of the model (2),

$$\frac{dS}{dt} = \Lambda - \phi_c IS - \mu S + \upsilon_3 R \geqslant \Lambda - (\phi_c I + \mu)S. \tag{3}$$

Using integrating factor, (3) can be expressed as

$$\frac{d}{dt}\left[S(t)e^{\int_0^t \phi_c I(s)\,\mathrm{d}s+\mu t}\right] \geqslant \Lambda\left(e^{\int_0^t \phi_c I(s)\,\mathrm{d}s+\mu t}\right).$$

Integrating both sides from $t=0$ to $t=t^*$ we obtain

$$\begin{aligned} S(t^*) &\geqslant S(0)\left(e^{-\int_0^{t^*}\phi_c I(s)\,\mathrm{d}s-\mu t^*}\right)+\left(e^{-\int_0^{t^*}\phi_c I(s)\,\mathrm{d}s-\mu t^*}\right) \\ &\times \int_0^{t^*}\Lambda\left(e^{\int_0^x \phi_c I(x)\,\mathrm{d}x+\mu y}\right)\mathrm{d}y \\ &> 0. \end{aligned} \tag{4}$$

From the result, $S(t^*)$ is greater than or equal to the sum of positive terms. By the same argument, we can also prove that

$$E(t)>0, I(t)>0, Q(t)>0, R(t)>0, \forall t^*>0. \quad \square$$

3.2. Boundedness of the solution

Theorem 2. *All solutions $S(0), E(0), I(0), Q(0), R(0)$ of the COVID-19 model in eq.(2) are bounded. That is, if*

$$\limsup_{t\to\infty} N(t) \leqslant \frac{\Lambda}{\mu},$$

then $N(t) = S(t) + E(t) + I(t) + Q(t) + R(t)$.

Proof. To prove boundedness of the solution, $0 < I(t) \leqslant N(t)$. Adding all the equations in model (2), we obtain

$$\frac{dN}{dt} = \Lambda - \mu N - \delta I. \tag{5}$$

The solutions of the proposed model in (2) are bounded. Hence, from eq.(5), $\Lambda-(\mu+\delta)N(t) \leqslant \frac{dN(t)}{dt} \leqslant \Lambda - \mu N(t)$. and this can now be written as

$$\frac{\Lambda}{(\mu+\delta)} \leqslant \liminf_{t\to\infty} N(t) \leqslant \limsup_{t\to\infty} N(t) \leqslant \frac{\Lambda}{\mu}. \quad \square \tag{6}$$

3.3. Invariant region of COVID-19 model

Considering COVID-19 model (2) with positive initial conditions, all the state variables must be feasible in the region Ω.

Theorem 3. *The region $\Omega \subset \mathbb{R}^5_+$ is non-negative invariant for the proposed model (2) with non-negative initial conditions $\mathbb{R}^5_+$.*

Proof. Let Ω denote the feasible region of the COVID-19 model in (2). Therefore, the feasible region of the COVID-19 model (2) can be expressed as $\Omega \subset \mathbb{R}^5_+$ with

$$\Omega = \left\{\left(S,E,I,Q,R\right) \in \mathbb{R}^5_+ : S+E+I+Q+R \leqslant \frac{\Lambda}{\mu}\right\}$$

The following steps are considered to verify the positive invariance of Ω that is, the solution in Ω still remains in $\Omega \forall t>0$. This follows that $\frac{dN(t)}{dt} \leqslant \Lambda - \mu N(t)$. By standard comparison theorem [32], we obtain

$$N(t) \leqslant N(0)e^{-\mu t} + \frac{\Lambda}{\mu}(1-e^{-\mu t}). \tag{7}$$

In particular, $N(t) \leqslant \frac{\Lambda}{\mu}$ if $N(0) \leqslant \frac{\Lambda}{\mu}$. Hence, the region Ω is positive invariant. It is sufficient to consider the dynamics of the flow formulated by model (2) in Ω. Therefore the COVID-19 model is well posed, Mathematically, Biologically and Epidemiologically valid in the region Ω. $\square$

3.4. Existence of equilibrium points for COVID-19 model

In this section, we examine the COVID-19 model (2) objectively with the condition of existence of the equilibrium points. To verify the existence of the equilibrium points, the COVID-19 free equilibrium (CFE) point can be obtained by setting the derivatives on the right-hand side equations of COVID-19 model (2) to be zero. It is also achieved by substituting humans infected with COVID-19 (I) to be zero. Thus,

$$E_0 = \left(\frac{\Lambda}{\mu}, 0, 0, 0, 0\right). \tag{8}$$

Similarly, setting the derivatives on the right-hand side of COVID-19 model (2) to be zero and substituting $S=S^*, E=E^*, I=I^*, Q=Q^*$ and $R=R^*$. Endemic equilibrium point (E_1) exists when I is non-zero and we obtain

$$\begin{aligned} S^* &= \frac{\Lambda+\upsilon_3 R^*}{\phi_c I^*+\mu}, \\ E^* &= \frac{\phi_c + I^* S^*}{(\sigma+\mu)}, \\ I^* &= \frac{\sigma E^* + \upsilon_1 R^*}{(\alpha+\upsilon_2+\delta+\mu)}, \\ Q^* &= \frac{\alpha I^*}{\theta+\mu}, \\ R^* &= \frac{\theta Q^* + \upsilon_2 I^*}{(\upsilon_1+\upsilon_3+\mu)}. \end{aligned} \tag{9}$$

By simplifying each of the equation in eq.(9) further to obtain

$$\begin{aligned} S^* &= \frac{a_2(a_1a_3a_4 - \alpha\theta\upsilon_1 - a_3\upsilon_1\upsilon_2)}{\phi_c\sigma a_3 a_4} \\ E^* &= \frac{(\Lambda\phi_c\sigma a_3a_4 + \alpha\mu\theta a_2\upsilon_1 - \mu a_1a_2a_3a_4 + \mu a_2a_3\upsilon_1\upsilon_2)}{(\alpha\sigma\theta\upsilon_3 + \alpha\theta a_2\upsilon_1 + \sigma a_3\upsilon_2\upsilon_3 - a_1a_2a_3a_4 + a_2a_3\upsilon_1\upsilon_2)} \times \frac{(\alpha\theta\upsilon_1 - a_1a_3a_4 + a_3\upsilon_1\upsilon_2)}{\phi_c\sigma a_3a_4} \\ I^* &= \frac{\mu a_1a_2a_3a_4 - \Lambda\phi_c\sigma a_3a_4 - \alpha\mu\theta a_2\upsilon_1 - \mu a_2a_3\upsilon_1\upsilon_2}{\phi_c(\alpha\sigma\theta\upsilon_3 + \alpha\theta a_2\upsilon_1 + \sigma a_3\upsilon_2\upsilon_3 - a_1a_2a_3a_4 + a_2a_3\upsilon_1\upsilon_2)} \\ Q^* &= \frac{\alpha(\mu a_1a_2a_3a_4 - \Lambda\phi_c\sigma a_3a_4 - \alpha\mu\theta a_2\upsilon_1 - \mu a_2a_3\upsilon_1\upsilon_2)}{\phi_c(\alpha\sigma\theta\upsilon_3 + \alpha\theta a_2\upsilon_1 + \sigma a_3\upsilon_2\upsilon_3 - a_1a_2a_3a_4 + a_2a_3\upsilon_1\upsilon_2)a_3} \\ R^* &= \frac{(\mu a_1a_2a_3a_4 - \Lambda\phi_c\sigma a_3a_4 - \alpha\mu\theta a_2\upsilon_1 - \mu a_2a_3\upsilon_1\upsilon_2)}{(\alpha\sigma\theta\upsilon_3 + \alpha\theta a_2\upsilon_1 + \sigma a_3\upsilon_2\upsilon_3 - a_1a_2a_3a_4 + a_2a_3\upsilon_1\upsilon_2)} \times \frac{(\alpha\theta + a_3\upsilon_2)}{\phi_c a_3a_4} \end{aligned} \tag{10}$$

where $a_1=(\alpha+\upsilon_2+\delta+\mu), a_2=(\sigma+\mu), a_3=(\theta+\mu)$ and $a_4=(\upsilon_1+\upsilon_3+\mu)$.

3.5. Basic Reproduction Number ($\mathscr{R}_0$) of COVID-19 Model

Whenever $\mathscr{R}_0 < 1$, each human discharges or liberates on average that is below one infected human then COVID-19 dies out. Otherwise, COVID-19 turns out to be endemic or affects the susceptible population. We derive $\mathscr{R}_0$ of the COVID-19 free equilibrium (CFE) by using next generation matrix approach [33,34]. Thus,

$$\mathbf{F} = \begin{pmatrix} 0 & \frac{\phi_c \Lambda}{\mu} & 0 \\ 0 & 0 & 0 \\ 0 & 0 & 0 \end{pmatrix}, \tag{11}$$

and

$$\mathbf{V} = \begin{pmatrix} (\sigma+\mu) & 0 & 0 \\ -\sigma & (\alpha+\upsilon_2+\delta+\mu) & 0 \\ 0 & -\alpha & (\theta+\mu) \end{pmatrix}. \tag{12}$$

Multiplying $\mathbf{F}$ with the inverse matrix of $\mathbf{V}$, the basic reproduction number ($\mathscr{R}_0$) is the dominant or largest eigenvalue corresponding to the Spectral radius of the matrix ($\mathbf{FV}^{-1}$). This is denoted by $\mathscr{R}_0 = \rho(\mathbf{FV}^{-1})$ where ρ is the Spectral radius. Therefore, the basic reproduction number is given by

$$\mathscr{R}_0 = \frac{\phi_c \Lambda \sigma}{\mu(\sigma+\mu)(\mu+\delta+\upsilon_2+\alpha)}. \tag{13}$$

3.6. Global Stability of the COVID-19 Free Equilibrium (CFE)

Theorem 4. *If $\mathscr{R}_0 < 1$ then the COVID-19 free equilibrium in eq.(8) is globally asymptotically stable. Otherwise, it is unstable.*

Proof. We define the Lyapunov function

$$\mathfrak{T} = x_1 E + x_2 I,$$

where $x_1 = \frac{\sigma}{(\alpha+\upsilon_2+\delta+\mu)(\sigma+\mu)}$ and $x_2 = \frac{1}{(\alpha+\upsilon_2+\delta+\mu)}$. It is easy to establish that x_1 and x_2 are positive. Differentiating $\mathfrak{T}$ with respect to time,

$$\dot{\mathfrak{T}} = x_1 \dot{E} + x_2 \dot{I},$$

$$\dot{\mathfrak{T}} = \left(\frac{\sigma}{(\alpha+\upsilon_2+\delta+\mu)(\sigma+\mu)}\right)\left(\phi_c IS - (\sigma+\mu)E\right) + \left(\frac{1}{(\alpha+\upsilon_2+\delta+\mu)}\right)\left(\sigma E - bI + \upsilon_1 R\right), \tag{14}$$

Simplifying eq.(14) to obtain

$$\dot{\mathfrak{T}} = \frac{\sigma\phi_c IS}{(\alpha+\upsilon_2+\delta+\mu)(\sigma+\mu)} + \frac{\upsilon_1 R}{(\alpha+\upsilon_2+\delta+\mu)} - I \leqslant \frac{\sigma\phi_c IS}{(\alpha+\upsilon_2+\delta+\mu)(\sigma+\mu)} - I, \tag{15}$$

This can be written as

$$\dot{\mathfrak{T}} = (\mathscr{R}_0 - 1)I. \tag{16}$$

From the result obtained in eq.(16), we can see that $\dot{\mathfrak{T}} \leqslant 0$ provided $\mathscr{R}_0 \leqslant 0$ as well as $\dot{\mathfrak{T}} = 0$ provided that $\mathscr{R}_0 = 1$ or $I = 0$. This implies that, the highest invariance set in $\{(S,E,I,Q,R) \in \mathbb{R}^5_+\}$ is the singleton DFE (E_0) and DFE (E_0) is globally asymptotically stable in $\mathbb{R}^5_+$ [35,36]. Epidemiologically, the proof of Theorem 4 show that, COVID-19 will die out in the neighbourhood whenever $\mathscr{R}_0 \leqslant 0$ regardless of the number in eq.(2) at the initial stage of the population. □

3.7. Global stability analysis of endemic equilibrium

Theorem 5. *If $\mathscr{R}_0 > 1$ then model (2) has a unique endemic equilibrium (E_1) whenever $\mathscr{R}_0 > 1$.*

Proof. The existence of endemic equilibrium points $E_1 = (S^*, E^*, I^*, Q^*, R^*)$ defined in eqs.(9) and (10), where I is written as

$$I^* = -\frac{\Lambda\phi_c\sigma a_3 a_4 + \alpha\mu\theta a_2\upsilon_1 - \mu a_1 a_2 a_3 a_4 + \mu a_2 a_3 \upsilon_1 \upsilon_2}{\phi_c(\alpha\sigma\theta\upsilon_3 + \alpha\theta a_2\upsilon_1 + \sigma a_3\upsilon_2\upsilon_3 - a_1 a_2 a_3 a_4 + a_2 a_3 \upsilon_1 \upsilon_2)} \tag{17}$$

By substitution method and making I subject of formula, eq.(17) becomes

$$\mathscr{A} I^* + \mathscr{B} = 0 \tag{18}$$

where $\mathscr{A} = \phi_c(\alpha\sigma\theta\upsilon_3 + \alpha\theta a_2\upsilon_1 + \sigma a_3\upsilon_2\upsilon_3 - a_1 a_2 a_3 a_4 + a_2 a_3 \upsilon_1 \upsilon_2)$ and $\mathscr{B} = \mu(a_1 a_2 a_3 a_4(\mathscr{R}_0 - 1) + \alpha\theta a_2\upsilon_1 + a_2 a_3 \upsilon_1 \upsilon_2)$. Hence, eq.(18) can be defined as $I_h^* = \frac{-\mathscr{B}}{\mathscr{A}} \leqslant 0$ if $\mathscr{B} \geqslant 0$ at $\mathscr{R}_0 \leqslant 1$, and endemic equilibrium does not exist. Moreover, $I_h^* = \frac{\mathscr{B}}{\mathscr{A}} > 0$ if $\mathscr{B} < 0$ at $\mathscr{R}_0 > 1$. Therefore, there exists the endemic equilibrium only at $\mathscr{R}_0 > 1$. This shows that model (2) has a unique endemic that is positive equilibrium whenever $\mathscr{R}_0 > 1$. □

Theorem 6. *If $\mathscr{R}_0 > 1$ then the endemic equilibrium of model (2) given by $E_1 = (S^*, E^*, I^*, Q^*, R^*)$ is globally asymptotically stable in the interior of the region $\mathbb{R}^5_+$.*

Proof. Following [35–37], the equation below is made of the following Goh-Volterra type Lyapunov function:

$$\mathscr{L} = S - S^* - S^* \ln\frac{S}{S^*} + E - E^* - E^* \ln\frac{E}{E^*} + k_1\left(I - I^* - I^* \ln\frac{I}{I^*}\right) + k_2\left(Q - Q^* - Q^* \ln\frac{Q}{Q^*}\right). \tag{19}$$

where $k_1 = \frac{\phi_c S^* I^*}{\sigma E^*}$ and $k_2 = \frac{\phi_c S^* I^*}{\alpha I^*}$. Differentiating eq.(19) with respect to time, we have;

$$\dot{\mathscr{L}} = \left(1 - \frac{S^*}{S}\right)\dot{S} + \left(1 - \frac{E^*}{E}\right)\dot{E} + \frac{\phi_c S^* I^*}{\sigma E^*}\left(1 - \frac{I^*}{I}\right)\dot{I} + \frac{\phi_c S^* I^*}{\alpha I^*}\left(1 - \frac{Q^*}{Q}\right)\dot{Q}. \tag{20}$$

If $R_h \to R_h^*$ as time, $t \to \infty$ in eq.(9) and model (2) then by using substitution method and simplifying to obtain,

$$\dot{\mathscr{L}} = \mu S^*\left(2 - \frac{S^*}{S} - \frac{S}{S^*}\right) + \phi_c S^* I^*\left(4 - \frac{S^*}{S} - \frac{I^* E}{I E^*} - \frac{S E^* I}{S^* E I^*} - \frac{I}{I^*} - \frac{Q}{Q^*} - \frac{I Q^*}{I^* Q}\right) \leqslant 0.$$

Lastly, since arithmetic mean is more than geometric mean, then the following inequalities hold;

$$2 - \frac{S^*}{S} - \frac{S}{S^*} \leqslant 0$$

and

$$4 - \frac{S^*}{S} - \frac{I^* E}{I E^*} - \frac{S E^* I}{S^* E I^*} - \frac{I}{I^*} - \frac{Q}{Q^*} - \frac{I Q^*}{I^* Q} \leqslant 0. \quad \square$$

Table 1
Description of Variables and Parameters of the model.

Variable	Description
$S(t)$	Number of susceptible humans at time t
$E(t)$	Number of exposed humans at time t
$I(t)$	Number of infectious humans at time t
$Q(t)$	Number of quarantine humans at time t
$R(t)$	Number of recovered humans at time t
$N(t)$	Total number of humans at time t
Control	**Description**
$u_1(t)$	Use of face mask, hand sanitizer and social distancing at time t
$u_2(t)$	Treatment of COVID-19 patients, active screening along with testing at time t
$u_3(t)$	Control against recurrence and reinfection of humans who have recovered from COVID-19 at time t
Parameter	**Description**
Λ	Recruitment rate of individuals
ϕ_c	Contact rate for COVID-19 Transmission
ω	Exposed rate of individuals
μ	Natural death rate
υ_2	Relapse rate of individuals
δ	COVID-19 death rate
θ	Recovery rate of COVID-19 from quarantine individuals
α	Detection rate of infectious individuals
υ_1	Recovery rate of COVID-19 from infectious individuals
υ_3	Rate at which recovered individuals returns back to susceptible class

Table 2
Value of parameters in the model.

Parameter	Value	Reference
Λ	750 day^{-1}	[10]
ϕ_c	0.0000124	Estimated
σ	0.000011618 day^{-1}	Estimated
μ	0.003324588	Fitted
υ_2	0.001466848 day^{-1}	Fitted
δ	0.00286	Estimated
θ	0.0766169 day^{-1}	Fitted
α	0.010939586 day^{-1}	Fitted
υ_1	0.1109289 day^{-1}	Fitted
υ_3	0.0022927 day^{-1}	Fitted
$\mathscr{R}_0$	0.523984	Calculated

Therefore, $\dot{\mathscr{L}} \leqslant 0$ for $\mathscr{R}_0 > 1$. Since all the parameters are positive with $\dot{\mathscr{L}} = 0$ provided that, $S = S^*, E = E^*, I = I^*, Q = Q^*$. Also $R \to R_h^*$ as time, $t \to \infty$ and by LaSalle's invariance principle [36], the endemic equilibrium E_1 is globally asymptotically stable whenever $\mathscr{R}_0 > 1$. Epidemiologically, the proof of Theorem 6 implies that, COVID-19 would establish itself in the neighbourhood whenever $\mathscr{R}_0 > 1$ regardless of the number of infectious humans at the initial stage of the population (see Table 1).

3.8. Model fitting and estimation of parameters

In this section, we carry out the numerical simulation for the model fitting using least square method. This enables us to compare our model with the daily data of COVID-19 released by NCDC from December 1, 2020, to January 31, 2020 as shown in Fig. 2. Also, we consider the NCDC report released on December 1, 2020, for the initial conditions $E(0) = 2003$ which is the sample tested, $I(0) = 416$ which is the new confirmed cases, $Q(0) = 404$ which is the quarantine of humans (that is, the differences between new confirmed cases and new confirmed fatalities), $R(0) = 115$ which is the new discharged cases and an estimated $S(0) = 5000$ which is the susceptible humans. using the initial conditions and some estimation of parameters (that is, ϕ_c, σ and δ), we are able to fit other parameters (that is, $\mu, \upsilon_1, \upsilon_2, \upsilon_3, \alpha$ and θ) as well as calculating the basic reproduction number $\mathscr{R}_0 = 0.523984$ in eq. (13) as shown in Table 2.

4. Optimal control analysis of COVID-19

Optimal control is one of the important tools used in mathematical biology to eradicate or minimize the rate of infection in exposed and infected humans in the population. In order to minimize COVID-19 transmission, we propose a model which is an extension of the model (1) by incorporating three control measures into the model. These are; Preventive effort being made by NCDC to ensure that the public follows the guidelines such as, use of face mask, hand sanitizer and social distancing ($u_1(t)$), treatment of COVID-19 patients, active screening along with testing ($u_2(t)$), and control against recurrence and reinfection of humans who have recovered from COVID-19 ($u_3(t)$). Therefore, the reduction rate of COVID-19 through NCDC guidelines is given by factor $(1 - u_1(t))$ and the new force of infection can be written as $\frac{(1-u_1(t))\phi_c I}{N}$. Also, reduction in relapse rate of humans who have recovered from COVID-19 is given by factor $(1 - u_3(t))$ and from the autonomous equations in eq.(1), the proposed optimal control of COVID-19 model can be written as

$$\begin{aligned}
\frac{dS}{dt} &= \Lambda - \frac{(1-u_1(t))\phi_c IS}{N} - \mu S + \upsilon_3 R,\\
\frac{dE}{dt} &= \frac{(1-u_1(t))\phi_c IS}{N} - (\sigma+\mu)E,\\
\frac{dI}{dt} &= \sigma E - (\alpha u_2(t) + \upsilon_2 + \delta + \mu)I + \upsilon_1(1-u_3(t))R,\\
\frac{dQ}{dt} &= \alpha u_2(t) I - (\theta+\mu)Q,\\
\frac{dR}{dt} &= \theta Q - (\upsilon_1(1-u_3(t)) + \upsilon_3 + \mu)R + \upsilon_2 I.
\end{aligned} \tag{21}$$

Following eq.(2), we normalize the above eq.(21) as

$$\begin{aligned}
\frac{dS}{dt} &= \Lambda - (1-u_1(t))\phi_c IS - \mu S + \upsilon_3 R,\\
\frac{dE}{dt} &= (1-u_1(t))\phi_c IS - (\sigma+\mu)E,\\
\frac{dI}{dt} &= \sigma E - (\alpha u_2(t) + \upsilon_2 + \delta + \mu)I + \upsilon_1(1-u_3(t))R,\\
\frac{dQ}{dt} &= \alpha u_2(t) I - (\theta+\mu)Q,\\
\frac{dR}{dt} &= \theta Q - (\upsilon_1(1-u_3(t)) + \upsilon_3 + \mu)R + \upsilon_2 I.
\end{aligned} \tag{22}$$

4.1. Description of Optimal Control

In this section, we minimize the total number of exposed and infected humans to COVID-19 in the population using the control variables $u_1(t)$, $u_2(t)$ and $u_3(t)$ in the model. Also, we show that all variables $u_1(t), u_2(t)$ and $u_3(t)$ in the model dynamics of the population are positive. According to [42], we define the objective function as

$$J = \int_0^{t_f} \left(A_1 E(t) + A_2 I(t) + \frac{1}{2}\left(B_1 u_1^2(t) + B_2 u_2^2(t) + B_3 u_3^2(t)\right)\right) \mathrm{d}t. \tag{23}$$

subject to model (22), where A_1 and A_2 are positive weight constants of exposed and infected humans respectively. B_1, B_2 and B_3 are positive weight constants of control variables $u_1(t), u_2(t)$ and $u_3(t)$ respectively. Meanwhile, the quadratic costs $B_1 u_1^2(t), B_2 u_2^2(t)$ and $P_3 u_3^2(t)$ associated

with the use of preventive effort by NCDC to ensure that the public follow the guidelines such as, use of face-mask, hand sanitizer along with social distancing, treatment of COVID-19 patients, active screening with testing and control against recurrence and reinfection of humans who have recovered from COVID-19 respectively. We choose the quadratic cost in line with the literature on epidemic controls [38–40]. The purpose is to find an optimal control of $u_1^*(t), u_2^*(t)$ and $u_3^*(t)$ such that;

$$J(u_1^*, u_2^*, u_3^*) = min\{(u_1, u_2, u_3) : u_1, u_2, u_3, \in \Omega\} \tag{24}$$

where $\Omega = \{u_i : 0 \leqslant u_i(t) \leqslant 1$, Lebesgue measurable $t = [0, t_f]$ for $i = 1, 2, 3\}$ is the control set subject to the model (22) with initial conditions.

4.2. Existence of the optimal control

In this part, we show the existence of the optimal control with initial conditions $t = 0$ viz state and prove the following theorems, and analyze the properties of the model (22) with all non-negative initial conditions $\forall t > 0$. We will also use model (22) to see the existence of optimal control with the necessary conditions that satisfy the Pontryagin's Maximum Principle [41]. This can be done by applying Pontryagin's Maximum Principle to convert Eqs. (22)–(24) into a problem of minimizing point-wise Lagrange, L, with respect to u_1, u_2 and u_3. The Lagrangian of the control problem is given by;

$$L = A_1 E(t) + A_2 I(t) + \frac{1}{2}\left[B_1 u_1^2(t) + B_2 u_2^2(t) + B_3 u_3^2(t)\right] \tag{25}$$

This would be used to find minimal value of the Lagrangian. It could be achieved by defining Hamiltonian, H, for the control problem as [41]

$$H = L + \lambda_1 \frac{dS(t)}{dt} + \lambda_2 \frac{dE(t)}{dt} + \lambda_3 \frac{dI(t)}{dt} + \lambda_4 \frac{dQ(t)}{dt} + \lambda_5 \frac{dR(t)}{dt}. \tag{26}$$

Substituting eq.(25) and model (22) into eq. (26), we obtain

$$\begin{aligned} H = {} & A_1 E(t) + A_2 I(t) + \frac{1}{2}\left[B_1 u_1^2(t) + B_2 u_2^2(t) + B_3 u_3^2(t)\right] + \lambda_1(\Lambda - (1 \\ & - u_1(t))\phi_c I(t) S(t) - \mu S(t) + \upsilon_3 R(t)) + \lambda_2((1 - u_1(t))\phi_c I(t) S(t) - (\sigma \\ & + \mu) E(t)) + \lambda_3(\sigma E(t) - (\alpha u_2(t) + \upsilon_2 + \delta + \mu) I(t) + \upsilon_1(1 \\ & - u_3(t)) R(t)) + \lambda_4(\alpha u_2(t) I(t) - (\theta + \mu) Q(t)) + \lambda_5(\theta Q - (\upsilon_1(1 - u_3(t)) \\ & + \upsilon_3 + \mu) R + \upsilon_2 I). \end{aligned} \tag{27}$$

Where $\lambda_1, \lambda_2, \lambda_3, \lambda_4$ and λ_5 are the adjoint variables.

The existence of optimal control of the model (22) would be considered by applying the theorem.

Theorem 7. *There exists an optimal control* $u^* = (u_1^*, u_2^*, u_3^*) \in \Omega$ *such that; the control model (22) with initial conditions at* $t = 0$ *and*

$$J(u_1^*, u_2^*, u_3^*) = min\{(u_1, u_2, u_3) : u_1, u_2, u_3 \in \Omega\} \tag{28}$$

Proof. The state and control variables of the model (22) are positive values and the control set Ω is close and convex. Therefore the integrand of the objective function J in which it is expressed in model (22) is a convex function of (u_1, u_2, u_3) on the control set Ω. Since the state solutions are bounded, then Lipschitz property of the state system with respect to the state variables is satisfied. It can also be seen that $\exists$ positive numbers η_1, η_2 and a constant $\epsilon > 1$ such that,

$$J(u_1, u_2, u_3) \geqslant \eta_1 \left(|u_1|^2 + |u_2|^2 + |u_3|^2\right)^{\epsilon/2} - \eta_2 \tag{29}$$

Therefore, the state variables are bounded and the existence of optimal control of the model (22) is concluded. □

4.3. Uniqueness of the optimal control

Pontryagin's Maximum Principle is used to reveal the necessary conditions for this optimal control. This is as a result of the fact that, minimizing the cost functional in eq. (23) subject to the model (22) is the existence of an optimal control. According to [19–21], If (x, u) is an optimal solution of an optimal control problem then $\exists$ a non-trivial vector function $\lambda = (\lambda_1, \lambda_2, \lambda_3, \lambda_4, \ldots, \lambda_n)$ thus, satisfying the following equations

$$\begin{aligned} \frac{dx}{dt} &= \frac{\partial H(t, x, u, \lambda)}{\partial \lambda}, \\ 0 &= \frac{\partial H(t, x, u, \lambda)}{\partial u}, \\ \lambda' &= \frac{\partial H(t, x, u, \lambda)}{\partial x}. \end{aligned} \tag{30}$$

Therefore, we can now apply the necessary conditions to the Hamiltonian, H, in eq.(27).

Theorem 8. *Let* S^*, E^*, I^*, Q^* *and* R^* *be optimal state solutions associated with optimal control* (u_1^*, u_2^*, u_3^*) *for the optimal control problem in model (22) and eq.(23). There exist the co-states* λ_i *which verify eq.(31) with the transversality conditions* $\lambda_i(t_f) = 0$ *in eq.(32) for* $i = 1, 2, 3, 4, 5$ *and in eq. (34) the control variables* (u_1^*, u_2^*, u_3^*).

Proof. Consider eq.(27) by differentiating Hamiltonian, H, with respect to S, E, I, Q and R. Also, considering the state variables by applying the first and third equations in eq.(30) into eq.(27), we have the following:

$$\begin{aligned} \frac{d\lambda_1}{dt} &= -\frac{\partial H}{\partial S} = ((1-u_1)\phi_c I)(\lambda_1 - \lambda_2) + \mu\lambda_1, \\ \frac{d\lambda_2}{dt} &= -\frac{\partial H}{\partial E} = \sigma(\lambda_2 - \lambda_3) + \mu\lambda_2 - A_1, \\ \frac{d\lambda_3}{dt} &= -\frac{\partial H}{\partial I} = ((1-u_1)\phi_c S)(\lambda_1 - \lambda_2) + \alpha u_2(\lambda_3 - \lambda_4) + \upsilon_2(\lambda_3 - \lambda_5) + (\delta + \mu)\lambda_3 - A_2, \\ \frac{d\lambda_4}{dt} &= -\frac{\partial H}{\partial Q} = \theta(\lambda_4 - \lambda_5) + \mu\lambda_4, \\ \frac{d\lambda_5}{dt} &= -\frac{\partial H}{\partial R} = \mu\lambda_5 - \upsilon_3(\lambda_1 - \lambda_5) - \upsilon_1(1-u_3)(\lambda_3 - \lambda_5). \end{aligned} \tag{31}$$

with the transversality conditions

$$\lambda_1(t_f) = \lambda_2(t_f) = \lambda_3(t_f) = \lambda_4(t_f) = \lambda_5(t_f) = \lambda_6(t_f) = \lambda_7(t_f) = 0 \tag{32}$$

To evaluate the optimal control of the control variable set, where $u_i = (0, 1)$. let $S = S^*, E = E^*, I = I^*, Q = Q^*$ and $R = R^*$ and apply the second equation in eq.(30) by differentiating Hamiltonian, H, in eq.(27) with respect to control variable u_1, u_2 and u_3 to obtain

$$\begin{aligned} \frac{\partial H}{\partial u_1} &= B_1 u_1^* - \phi_c I^* S^*(\lambda_2 - \lambda_1) = 0, \\ \frac{\partial H}{\partial u_2} &= B_2 u_2^* - \alpha I^*(\lambda_3 - \lambda_4) = 0, \\ \frac{\partial H}{\partial u_3} &= B_3 u_3^* - \upsilon_1 R^*(\lambda_3 - \lambda_5) = 0, \end{aligned} \tag{33}$$

make u_i^* for $i = 1, 2, 3$ subject of formula to obtain

$$\begin{aligned} u_1^* &= \left(\frac{\phi_c I^* S^*(\lambda_2 - \lambda_1)}{B_1}\right), \\ u_2^* &= \left(\frac{\alpha I^*(\lambda_3 - \lambda_4)}{B_2}\right), \\ u_3^* &= \left(\frac{\upsilon_1 R^*(\lambda_3 - \lambda_5)}{B_3}\right). \end{aligned}$$

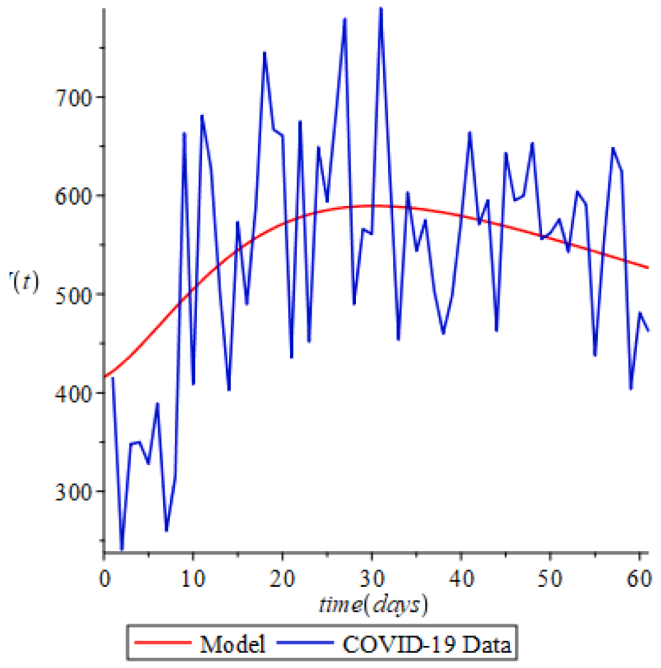

Fig. 3. Graph of COVID-19 Data and Model.

Therefore, we have

$$u_1^* = max\left\{0, min\left(\frac{\phi_c I^* S^* (\lambda_2 - \lambda_1)}{B_1}\right)\right\},$$
$$u_2^* = max\left\{0, min\left(\frac{\alpha I^* (\lambda_3 - \lambda_4)}{B_2}\right)\right\}, \quad (34)$$
$$u_3^* = max\left\{0, min\left(\frac{\upsilon_1 R^* (\lambda_3 - \lambda_5)}{B_3}\right)\right\}.$$

This show that, the uniqueness of the optimal control of the model has been achieved for small t_f based on prior boundedness of the state variables as well as adjoint variables. This is made possible through the use of Lipschitz property of the ordinary differential equations. Graph of COVID-19 data and model is provided in Fig. 3. □

4.4. Numerical Solution of the Optimal Control

The optimality system consists of state system in eq.(22), optimal control set in eq.(32), adjoint system in eq.(31), boundary conditions in eq.(31) and initial conditions according to NCDC report on December 1, 2020, the initial conditions are $E(0) = 2003, I(0) = 416, Q(0) = 404$, $R(0) = 115$ with estimated $S(0) = 5000$ (estimated), weight constants $B_1 = 19, B_2 = 1, P_1 = 0.07, P_2 = 0.05$ and $P_3 = 0.03$. Using this optimality system, the state variables and optimal control can be calculated. It shows that, the second equation in eq.(30) applied on Hamiltonian eq. (27) is positive which means optimal problem is minimal at controls u_1^*, u_2^* and u_3^*. Replacing eq.(34) into the model (22), we have;

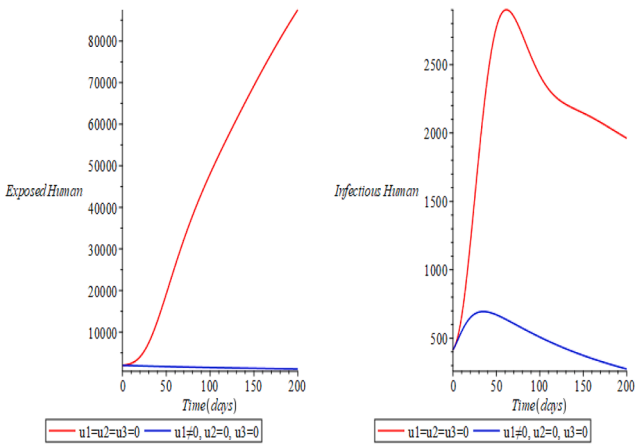

(a) Optimal Control graph of Exposed Humans against Time.

(b) Optimal Control graph of Infected Humans against Time.

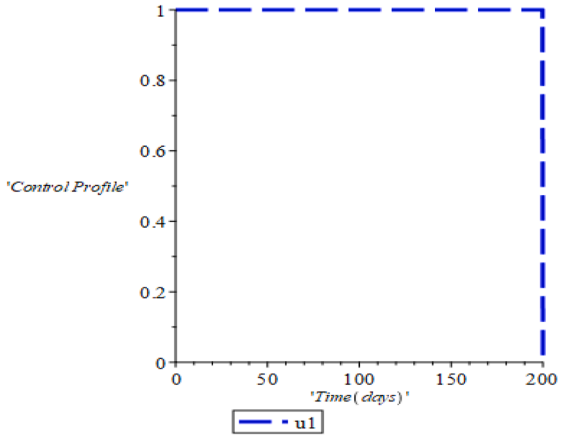

(c) Control Profile graph of $u_1(t)$ againstTime.

Fig. 4. Simulation of COVID-19 Optimal Control model showing the impact of using face-mask on humans $u_1(t)$.

$$\frac{dS}{dt} = \Lambda - (1 - max\{0, min(1, \mathfrak{B}_1)\})\phi_c IS - \mu S + \upsilon_3 R,$$
$$\frac{dE}{dt} = (1 - max\{0, min(1, \mathfrak{B}_1)\})\phi_c IS - (\sigma + \mu)E,$$
$$\frac{dI}{dt} = \sigma E - (\alpha(max\{0, min(1, \mathfrak{B}_2)\}) + \upsilon_2 + \delta + \mu)I + \upsilon_1(1 - max\{0, min(1, \mathfrak{B}_3)\})R,$$
$$\frac{dQ}{dt} = \alpha(max\{0, min(1, \mathfrak{B}_2)\})I - (\theta + \mu)Q,$$
$$\frac{dR}{dt} = \theta Q - (\upsilon_1(1 - max\{0, min(1, \mathfrak{B}_3)\}) + \upsilon_3 + \mu)R + \upsilon_2 I. \quad (35)$$

where $\mathfrak{B}_1 = \left(\frac{\phi_c I^* S^* (\lambda_2 - \lambda_1)}{B_1}\right), \mathfrak{B}_2 = \left(\frac{\alpha I^* (\lambda_3 - \lambda_4)}{B_2}\right),$
$\mathfrak{B}_3 = \left(\frac{\upsilon_1 R^* (\lambda_3 - \lambda_5)}{B_3}\right).$

4.5. Graphical solution of the optimal control

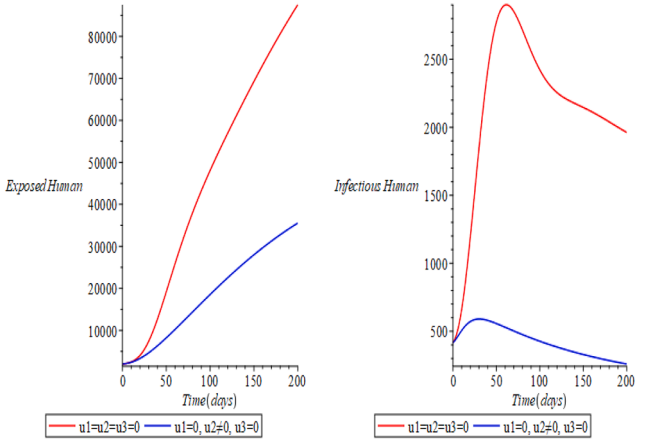

(a) Optimal Control graph of Exposed Humans against Time.

(b) Optimal Control graph of Infected Humans against Time.

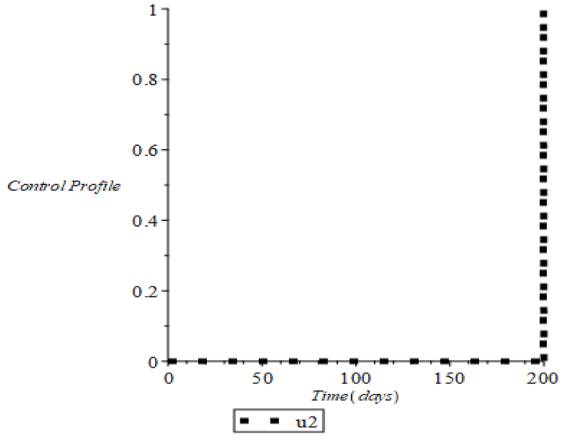

(c) Control Profile graph of $u_2(t)$ againstTime.

Fig. 5. Simulation of COVID-19 Optimal Control model showing the impact of treatment on COVID-19 patients $u_2(t)$.

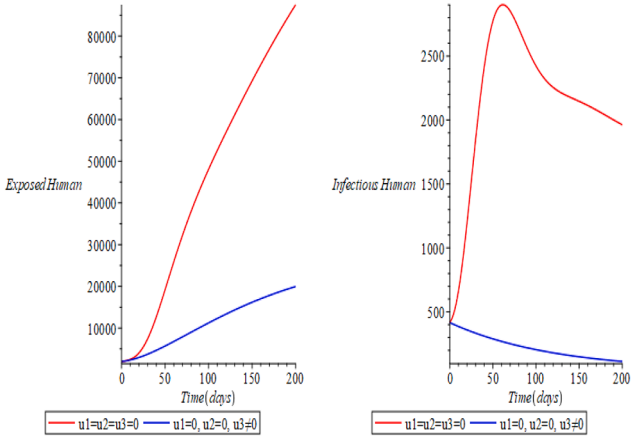

(a) Optimal Control graph of Exposed Humans against Time.

(b) Optimal Control graph of Infecte Humans against Time.

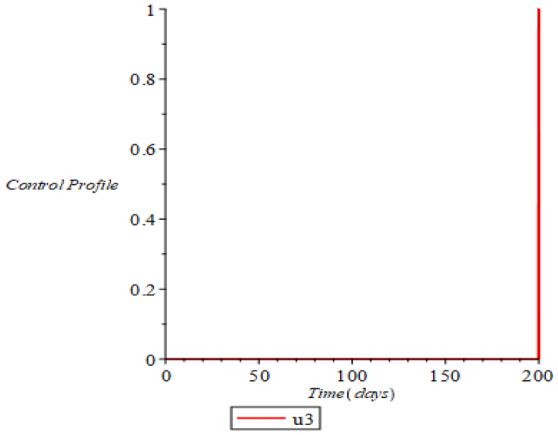

(c) Control Profile graph of $u_3(t)$ against Time.

Fig. 6. Simulation of COVID-19 Optimal Control model showing the impact of control against relapse on humans who have recovered from COVID-19 ($u_3(t)$).

5. Discussion of the Results

5.1. Category A: Use of face-mask, sanitizer and keeping social distancing control

In this category, Fig. 4 illustrates the impact of face-mask, sanitizer and social distancing control (u_1) in eradicating COVID-19 in Nigeria. As shown in Fig. 4 that is, in Fig. 4(a), it is shown that, the number of exposed humans increases from 2003 very fast above 87509 at time t = 200 days when the use of face-mask, sanitizer and social distancing control are not implemented. But when the use of face-mask, sanitizer and social distancing control are implemented, it decreases gradually from 2003 to 1132 at time t = 200 days and it will continue to decrease until there is no exposed humans as time increases. Fig. 4(b) shows that the number of infected humans increases from 416 very fast until it reaches 2899 within time t = 52 days before gradual reduction of number of infected humans when the use face-mask, sanitizer and social distancing control is not implemented. But when the use of face-mask, sanitizer and social distancing control is implemented, the number of infected humans increases gradually from 416 until it reaches 692 within time t = 30 days before decreasing gradually until there is no infected humans as time increases. The control profile in Fig. 4(c) shows that, the use of face-mask, sanitizer and social distancing control (u_1) is at its maximum value from the starting point until time t = 200 days before decreasing to the minimum value.

5.2. Category B: Treatment of COVID-19 patients, active screening and testing

In this category, Fig. 5 shows the influence of treatment of COVID-19 patients, active screening and testing control (u_2) on COVID-19 spread in Nigeria. As shown in Fig. 5 that is, in Fig. 5(a), it is verified that the number of exposed humans keeps on increasing from 2003 very fast above 87510 at time t = 200 days in the absence of treatment of COVID-19 patients control. Also, when it involves treatment of COVID-19 patients, active screening and testing control, the number of exposed human increases from 2003 not as fast as without control above 35545 at time t = 200 days. In Fig. 5(b), it is verified that the number of infected humans increases from 416 very fast until it reaches 2899 within time t = 52 days before gradual reduction of number of infected humans when treatment of COVID-19 patients, active screening and testing control is not implemented. But when the treatment of COVID-19 patients, active screening and testing control are implemented, it increases gradually from 416 until it reaches 580 within time t = 30 days before decreasing gradually until there is no infected human as time increases. The control profile in Fig. 5(c) show that, treatment of COVID-19 patients, active screening and testing control (u_2) is at its minimum

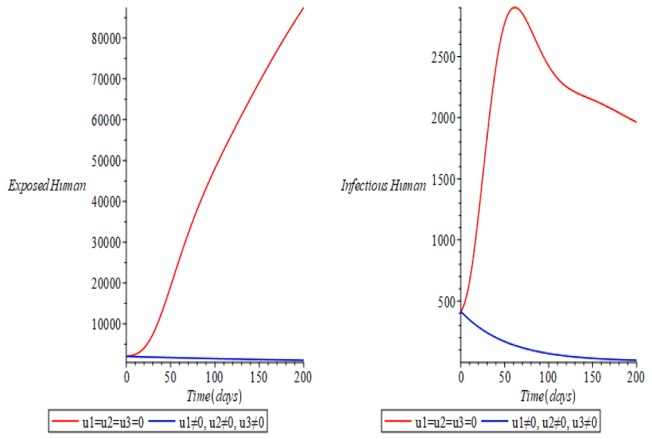

a) Optimal Control graph of Exposed Humans against Time.

(b) Optimal Control graph of Infected Humans against Time.

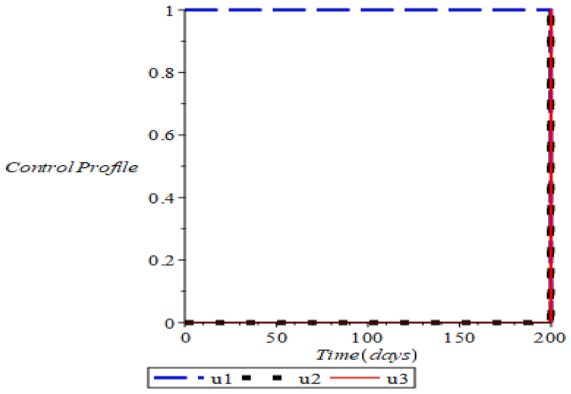

(c) Control Profiles graph of $u_1(t)$, $u_2(t)$ and $u_3(t)$ against Time

Fig. 7. Simulation of COVID-19 Optimal Control model showing the impact of using face-mask on humans $(u_1(t))$, treatment on COVID-19 patients, active screening and testing $(u_2(t))$ and control against recurrence and reinfection of humans who have recovered from COVID-19. $(u_3(t))$.

value from the starting point until time t = 200 days before increasing to the maximum value.

5.3. Category C: Control against recurrence and reinfection of humans who have recovered from COVID-19

In this category, Fig. 6 shows the effect of control against relapse of humans who have recovered from COVID-19 (u_3). From Fig. 6 that is, in Fig. 6(a), it is confirmed that the number of exposed human continue to increase very rapid above 87509 at time t = 200 days without the control against relapse of humans who have recovered from COVID-19. But with the control against relapse of humans who have recovered from COVID-19, the number of exposed humans increases from 2003 gradually above 19957 at time t = 200 days. In Fig. 6(b), it is confirmed that the number of infected humans increases from 416 very fast until it reaches 2899 within time t = 52 days before gradual reduction of the number of infected humans without the implementation of control against relapse of humans who have recovered from COVID-19. But with the implementation of control against relapse of humans who have recovered from COVID-19, it decreases gradually from 416 to 112 at time t = 200 days and it will continue to decrease until there is no infected human as time increases. The control profile in Fig. 6(c) shows that, the control against relapse of humans who have recovered from COVID-19 (u_3) is at its minimum value from the starting point until time t = 200 days before increasing to the maximum value.

5.4. Category D: Use of face-mask, sanitizer and keeping social distancing control, treatment of COVID-19 patients, active screening and testing, and control against relapse of humans who have recovered from COVID-19

In this category, Fig. 7 shows the impact of face-mask, sanitizer and social distancing control (u_1), treatment of COVID-19 patients, active screening and testing (u_2), and control against relapse of humans who have recovered from COVID-19 (u_3). As shown in Fig. 7 that is, in Fig. 7 (a), it is verified that the number of exposed human increases from 2003 very fast above 87509 at time t = 200 days without control strategies (u_1, u_2 and u_3). But with control strategies (u_1, u_2 and u_3), the number of exposed human decreases gradually from 2003 to 1042 at time t = 200 days and it will continue to decrease until there is no exposed human as time increases. In Fig. 7(b), it is verified that the number of infected human increases from 416 very fast until it reaches 2899 within time t = 52 days before gradual reduction of number of infected humans when all the control strategies (u_1, u_2 and u_3) are not implemented, but when all the control strategies (u_1, u_2 and u_3) are implemented, it decreases gradually from 416 to 15 at time t = 200 days and it will continue to decrease until there is no infected humans as time increases. The control profile in Fig. 7(c) shows that, use of face-mask, sanitizer and social distancing control (u_1) is at its maximum value from the starting point until time t = 200 days before decreasing to the minimum value. Also, treatment of COVID-19 patients, active screening along with testing (u_2), and control against recurrence and reinfection of humans who have recovered from COVID-19. (u_3) are at their minimum values from the starting point until time t = 200 days before increasing to their maximum values.

6. Conclusion

Mathematical study on the transmission dynamics of the novel COVID-19 pandemic was discussed in order to provide more insights into disease transmission, explore potential prevention and control strategies to minimize the rising tide of disease transmission in the population. A deterministic mathematical model was formulated by subdividing the human population into susceptible human, exposed human, infected human, quarantine human and recovered human. The theoretical study carried out on the basis of the stability analysis showed that the model has a globally asymptotically stable disease-free equilibrium if the basic number of reproductions of new transmissions of coronaviruses is less than one. The biological interpretation of this findings revealed that:

- COVID-19 can be effectively managed or even eliminated if the control measures implemented are capable of taking or sustaining the basic reproductive number R_0 to a value below unity. This is an indication that, regardless of the number of infectious individuals initially introduced into the fully susceptible population.
- The spread of COVID-19 in the population can be efficiently managed. In addition, three separate simulation cases were conducted to obtain the best control strategies in a comparative manner.
- The results from our analysis revealed that the impacts of three interventions with optimal implementation costs out-perform the reduction of the disease epidemic.

Therefore, the fight against the spread of COVID-19 requires a multifaceted approach. We have not considered other control measures such as personal hygiene and public awareness, this gives space for future research. The findings obtained in this work can be a valuable reference for COVID-19 Local National Control Program and the basis for the preparation and design of the best intervention strategies to eradicate COVID-19.

CRediT authorship contribution statement

Adesoye Idowu Abioye: Conceptualization, Resources, Writing - review & editing. **Olumuyiwa James Peter:** Conceptualization, Resources, Visualization, Writing - review & editing. **Hammed Abiodun Ogunseye:** Data curation, Methodology, Validation, Visualization, Writing - original draft. **Festus Abiodun Oguntolu:** Formal analysis, Supervision. **Kayode Oshinubi:** Data curation, Validation, Writing - original draft. **Abdullahi Adinoyi Ibrahim:** Formal analysis, Methodology, Project administration, Software, Supervision. **Ilyas Khan:** Funding acquisition, Project administration, Software.

Declaration of Competing Interest

The authors declare that they have no known competing financial interests or personal relationships that could have appeared to influence the work reported in this paper.

References

[1] Rothana HA, Byrareddy SN. The epidemiology and pathogenesis of coronavirus disease (COVID-19) outbreak. J Autoimmun 2020;109:102433.
[2] WHO. 2020. https://www.who.int/emergencies/diseases/novel-coronavirus-2019. Accessed 7 May 2020.
[3] Cucinotta D, Vanelli M. WHO Declares COVID-19 a Pandemic. Acta Biomed 2020; 91(1):157–60. https://doi.org/10.23750/abm.v91i1.9397.
[4] Corona Virus Live Tracker. [Online]. Available:https://www.corona.tuply.co.za. Accessed 7 September 2020.
[5] Akinyemi AI, Isiugo-Abanihe UC. Demographic dynamics and development in nigeria. African Population Studies 2014;27:239–48.
[6] First case of corona virus disease confirmed in nigeria, 2020. URL: https://ncdc.gov.ng/news/ 227/first-case-of-corona-virus-disease-confirmed-in-nigeria.
[7] NCDC, Nigeria Center for Disease Control. [Online]. Available: http://covid19.ncdc.gov.ng/. Accessed 7 September 2020.
[8] Madubueze CE, Kimbir AR, Aboiyar T. Global Stability of Ebola Virus Disease Model with Contact Tracing and Quarantine. Appl Appl Math 2018;13(1):382–403.
[9] Kim Y, Lee S, Chu C, Choe S, Hong S, Shin Y. The characteristics of middle eastern respiratory syndrome coronavirus transmission dynamics in South Korea. Osong Public Health Res Perspectives 2016;7(1):49–55.
[10] Krishna MV, Prakash J. Mathematical modelling on phase based transmissibility of corona virus. Infect Dis Model 2020;5:375–85. 3A.
[11] Kucharski J, Russell TW, Diamond C, Liu Y, Edmunds J, Funk S, et al. Early dynamics of transmission and control of COVID-19: a mathematical modelling study. Lancet Infect Dis 2020;20:553–8. https://doi.org/10.1016/S1473-3099(20)30144-4.
[12] Emile F. Doungmo Goufo, Y. Khan, Qasim A. Chaudhry. HIV and shifting epicenters for COVID-19, an alert for some countries. Chaos, Solitons & Fractals. Vol 139, October 2020, 110030. doi: 10.1016/j.chaos.2020.110030.
[13] A. Atangana, S. İğret Araz. Mathematical model of COVID-19 spread in Turkey and South Africa: theory, methods, and applications. Adv Differ Equ 2020, 659 (2020). doi: 10.1186/s13662-020-03095-w.
[14] Faraz N, Khan Y, Goufo E, Anjum A, Anjum A. Dynamic analysis of the mathematical model of COVID-19 with demographic effects. Zeitschrift fur Naturforschung. C. J Biosci 2020;75(11–12):389–96. https://doi.org/10.1515/znc-2020-0121.
[15] Sookaromdee P, Wiwanitkit V. Imported cases of 2019-novel coronavirus (2019-ncov) infections in Thailand: Mathematical modelling of the outbreak. Asian Pac J Trop Med 2020;13:139–40. https://doi.org/10.4103/1995-7645.277516.
[16] Cakir Z, Savas H. A mathematical modelling approach in the spread of the novel 2019 coronavirus sars-cov-2 (COVID-19) pandemic. Electron J Gen Med 2020;17: em205. https://doi.org/10.29333/ejgm/7861.
[17] V. Volpert, M. Banerjee, S. Petrovskii, On a quarantine model of coronavirus infection and data analysis, Math. Model. Nat. Phenom., 15, 24.
[18] Khrapov P, Loginova A. Mathematical modelling of the dynamics of the coronavirus COVID-19 epidemic development in China. Int J Open Inf Tech 2020; 8:13–6.
[19] Peter OJ, Viriyapong R, Oguntolu FA, Yosyingyong P, Edogbanya HO, Ajisope MO. Stability and optimal control analysis of an SCIR epidemic model. J Math Computer Sci 2020;10:2722–53. https://doi.org/10.28919/jmcs/5001.
[20] Ayoade AA, Peter OJ, Ayoola TA, Amadiegwu S, Victor AA. Optimal Intervention Strategies for Transmission Dynamics of Cholera Disease. Malaysian J Appl Sci 2019;4(1):26–37.
[21] Zamir M, Abdeljawad T, Nadeem F, Wahid A, Yousef A. An optimal control analysis of a COVID-19 model. Alexandria Eng J 2021;60(3):2875–84. https://doi.org/10.1016/j.aej.2021.01.022.
[22] He S, Tang S, Rong L. A discrete stochastic model of the COVID-19 outbreak: Forecast and control. Math Biosci Eng 2020;17:2792–804. https://doi.org/10.3934/mbe.2020153.
[23] Peter OJ, Qureshi S, Yusuf A, Shomrani M, Idowu AA. A new mathematical model of COVID-19 using real data from Pakistan. Results Phys 2021;24:104098. https://doi.org/10.1016/j.rinp.2021.104098.
[24] Peter OJ, Shaikh AS, Ibrahim MO, Nvisar KS, Baleanu D, Khan I, Abioye AI. Analysis and Dynamics of Fractional Order Mathematical Model of COVID-19 in Nigeria Using Atangana-Baleanu Operator. Computers, Mater Continua 2021;66 (2):1823–48. https://doi.org/10.32604/cmc.2020.012314.
[25] A.I Abioye, M.D. Umoh, O.J. Peter, H.O. Edogbanya3, F.A. Oguntolu, O. Kayode, S. Amadiegwu. Forecasting of COVID-19 Pandemic in Nigeria Using Real Statistical Data. Communication in Mathematical Biology and Neurosciences. 2021 (2021) Article ID 2. https://doi.org/10.28919/cmbn/5144.
[26] Zhao H, Feng Z. Staggered release policies for COVID-19 control: Costs and benefits of relaxing restrictions by age and risk. Math Biosci 2020;326:108405. https://doi.org/10.1016/j.mbs.2020.108405.
[27] Yang C, Wang J.A mathematical model for the novel coronavirus epidemic in Wuhan, China, Mathematical Biosciences and Engineering, 17(3), 2708–2724.
[28] Atangana A. Modelling the spread of COVID-19 with new fractal-fractional operators: Can the lockdown save mankind before vaccination? Chaos Solitons Fractals 2020;136:109860.
[29] Okuonghae D, Omame A. Analysis of a mathematical model for COVID-19 population dynamics in Lagos, Nigeria, Chaos. Solitons and Fractals 2020. https://doi.org/10.1016/j.chaos.2020.110032.
[30] Ayinde K, Lukman AF, Rauf RI, et al. Modeling Nigerian Covid-19 cases: A comparative analysis of models and estimators. Chaos, Solitons Fractals 2020;138: 109911.
[31] Abdulmajeed K, Adeleke M, Popoola L. Online forecasting of COVID-19 cases in Nigeria using limited data. Data in Brief 2020;30:105683. https://doi.org/10.1016/j.dib.2020.105683.
[32] Lakshmikantham V, Leela S, Martynyuk AA. Stability Analysis of Nonlinear Systems. New York and Basel: Marcel Dekker Inc; 1989. https://doi.org/10.1007/978-3-319-27200-9.
[33] Liu Y, Gayle AA, Wilder-Smith A, Rocklöv J. The reproductive number of COVID-19 is higher compared to SARS coronavirus. J Travel Med 2020:1–4. https://doi.org/10.1093/jtm/taaa021.
[34] van den Driessche P, Watmough J. Reproduction numbers and sub-threshold endemic equilibria for compartmental models of disease transmission. Math Biosci 2002;180:29–48.
[35] A.I. Abioye, O.J. Peter, F.A. Oguntola, A.F. Adebisi, T.F. Aminu, Global stability of SEIR-SEI) model of malaria, Adv. Math. Sci. Journal, 9(8), 5305–5317.
[36] La Salle J, Lefschetz S. The Stability of Dynamical Systems. Philadelphia: SIAM; 1976.
[37] Peter OJ, Adebisi AF, Ajisope MO, Ajibade FO, Abioye AI, Oguntolu FA. Global Stability Analysis of Typhoid Fever Model. Adv Syst Sci Appl 2020;20:20–31. https://doi.org/10.25728/assa.2020.20.2.792.
[38] Peter OJ, Abioye AI, Oguntolu FA, Owolabi TA, Ajisope MO, Zakari AG, Shaba TG. Modelling and Optimal control analysis of Lassa fever disease. Informatics Med Unlocked 2020;20:100419. https://doi.org/10.1016/j.imu.2020.100419.
[39] Romero-Leiton JP, Montoya-Aguilar JM, Ibargöen-Mondragón E. An Optimal Control Problem Applied to Malaria Disease in Colombia. Appl Math Sci 2018;12 (6):279–92. https://doi.org/10.12988/ams.2018.819.
[40] Abioye AI, Ibrahim MO, Peter OJ, Ogunseye HA. Optimal control on a mathematical model of malaria. Sci Bull, Series A: Appl Math Phy 2020:178–90.
[41] Pontryagin LS, Boltyanskii VG, Gamkrelidze RV, Mishchenko EF. The Mathematical Theory of Optimal Processes. New York: Wiley; 1962.
[42] S. Lenhart, J.T. Workman, J.T. Optimal Control Applied to Biological Models. Chapman & Hall, Boca Raton, (2007).